Applied Physics Letters

# Device quality templates of $In_xGa_{1-x}N$ ($x < 0.1$) with defect densities comparable to GaN

Cite as: Appl. Phys. Lett. **117**, 052103 (2020); https://doi.org/10.1063/5.0015419
Submitted: 27 May 2020 . Accepted: 24 July 2020 . Published Online: 06 August 2020

Evyn L. Routh, Mostafa Abdelhamid, N. A. El-Masry, and S. M. Bedair

Applied Physics Letters ARTICLE scitation.org/journal/apl

# Device quality templates of $In_xGa_{1-x}N$ ($x < 0.1$) with defect densities comparable to GaN

Cite as: Appl. Phys. Lett. **117**, 052103 (2020); doi: 10.1063/5.0015419
Submitted: 27 May 2020 · Accepted: 24 July 2020 ·
Published Online: 6 August 2020



Evyn L. Routh,[1,a)] Mostafa Abdelhamid,[2] N. A. El-Masry,[1,3] and S. M. Bedair[2]

## AFFILIATIONS

[1]Department of Materials Science and Engineering, North Carolina State University, Raleigh, North Carolina 27695, USA
[2]Department of Electrical and Computer Engineering, North Carolina State University, Raleigh, North Carolina 27695, USA
[3]National Science Foundation, Alexandria, Virginia 22314, USA

[a)]Author to whom correspondence should be addressed: ellee2@ncsu.edu

## ABSTRACT

InGaN/GaN multiple quantum well (MQW) structures currently used in optical devices are based on highly strained InGaN films. The presence of strain reduces quantum efficiency and indium incorporation, two critical parameters in addressing the green gap. We report on the growth of InGaN-relaxed templates on GaN as substrates to reduce the strain in the MQW structures. Relaxation in the InGaN templates, due to the lattice mismatch, is accommodated by the generation of *V-pits* rather than the formation of misfit dislocations. $In_xGa_{1-x}N$ templates ($x \sim 0.1$) are grown via a modified semibulk (SB) approach, with a gradually increasing GaN interlayer thickness to provide a mechanism for backfilling of *V-pits*. We used high-resolution x-ray diffraction rocking curves to quantify the edge-type and screw-type dislocation density present in the SB and compared the results with the etch pit density obtained via atomic force microscopy after treating the SB with a silane etch. Device-quality InGaN templates with defect density in the mid $10^8\,cm^{-2}$ were investigated using the above two approaches, with a quality comparable to state-of-the-art GaN.



Traditionally, InGaN/GaN multiple quantum wells (MQWs) are grown on a sapphire wafer with a GaN buffer. However, the large lattice mismatch between InN and GaN (up to 11%) can prove to be challenging for device performance as the large lattice mismatch produces a compressive strain in the QWs, diminishing the performance of the device.[1,2] The strain becomes especially prevalent in increasing values of x where emission ranges from green to red. This has colloquially been deemed the "green gap problem."[1,2] Ideally, InGaN-based structures are to be grown on InGaN templates, which are nearly lattice matched to avoid the harmful effect of strain. However, such templates grown as bulk InGaN on GaN face several problems, such as rough surfaces, high densities of *V-pits*, high density of threading dislocations ($10^9$–$10^{10}\,cm^{-2}$ range), metal inclusions, and stacking faults.[3–6] In addition, earlier effort on InGaN templates was limited to very low values of x in $In_xGa_{1-x}N$, strained films, or highly defective templates.[3,7–9]

Threading dislocations (TDs) arise from the interface of InGaN templates grown on GaN due to the lattice mismatch, which propagate into the device region.[7,10,11] These defects are present in the form of edge-, screw-, and mixed-type dislocations.[12] Also, *V-pits* have been shown to form at the termination of TDs at a free surface in InGaN to release some of the strain present in the films.[7,11,12] *V-pits*, with the density in the $10^9\,cm^{-2}$ range, present as six-sided hexagonal shaped pits oriented toward the (0001) surface with faces on the {10–11} planes.[7,11,12] We have recently shown via transmission electron microscopy (TEM) studies that, for $In_xGa_{1-x}N$ ($x < 0.1$) templates grown on GaN, relaxation due to the lattice mismatch can be accommodated by the formation of *V-pits* rather than the formation of new misfit dislocations.[13] However, these high densities of *V-pits* and dislocations will impact the device performances based on MQW structures grown on these templates.

To circumvent the lattice mismatch problem in InGaN grown on GaN, a semibulk (SB) template approach is used.[14] The usage of SB by our group is discussed elsewhere.[14] The SB contains 20–30 periods of low temperature InGaN with 1–2 nm thick GaN interlayers grown on commercially supplied GaN substrates. We have also shown that these *V-pits* can be refilled by the GaN interlayers during the SB growth processes, thus rendering a smooth top surface.[13] However, for thick templates grown by the SB, we observed that for a high degree of relaxation, the *V-pits* get larger in size on the surface and become very deep, and the GaN interlayer filling process is not efficient, resulting in rough surfaces. As we have shown earlier, the degree of relaxation as

well as the size of the *V-pits* increases with the film thickness during the SB growth and relaxation processes.[13,14]

In the current work, we modified the SB growth by gradually increasing the GaN interlayer thickness to increase the chances of filling these *V-pits* specifically for the topmost layers of the InGaN templates where higher degrees of relaxation are taking place. By increasing the GaN interlayer thickness as the SB growth proceeds, the SB film is able to relax via *V-pit* formation without sacrificing the surface morphology, as the GaN interlayer provides a mechanism of back filling. Such an approach will result in templates with both smooth surfaces and low dislocation densities (mid $10^8$ cm$^{-2}$) since the relaxation due to the lattice mismatch between the InGaN and GaN substrates is accommodated by the *V-pit* formation rather than new misfit dislocations. Dussaigne *et al.* have shown the ability to decrease the number of existing *V-pits* by increasing the thickness of the GaN interlayer in pseudomorphic InGaN/GaN superlattices grown on InGaN pseudo-substrates.[15] The current approach is compatible with Metal-Organic Chemical Vapor Deposition (MOCVD) growth of large area InGaN templates that will be the substrates for MQW device structures.

Semibulk (SB) samples were grown on 300 $\mu$m n-type GaN on sapphire substrates supplied commercially (dislocation density $\sim 10^8$ cm$^{-2}$) via MOCVD, as was previously reported by Abdelhamid *et al.*[14] The conventional SB, shown in Fig. 1(a), is made of 18 nm $In_xGa_{1-x}N$ growth, followed by an ~2 nm thick GaN interlayer over the entire structure.

In this work, three SB samples were studied. A schematic for the microstructure for the samples can be seen in Fig. 1. For sample A (conventional SB), the GaN interlayer thickness "t" was fixed at ~2 nm, as seen in Fig. 1(a). For samples B–C, the GaN interlayer varied in thickness as the periods progressed; for the first 15 periods, the GaN interlayer target thickness was 2 nm, followed by gradually increasing the GaN interlayer thickness every 3 periods until 30 periods were reached, as seen in Fig. 1(b). The final thickness of the GaN interlayer for samples B–C in the last three periods was ~3.5 nm.

The indium content in the SB was controlled by temperature and verified via photoluminescence (PL) measurements using a 325 nm He–Cd laser. Samples A and B have the same growth temperature

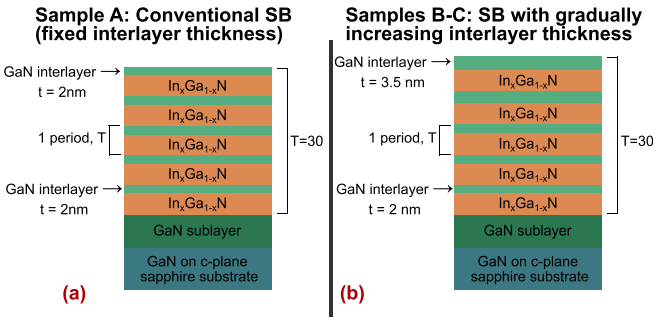


**FIG. 1.** Schematic representation of the $In_xGa_{1-x}N$/GaN semibulk (SB) microstructure, where one period is equal to an $In_xGa_{1-x}N$ layer and a GaN interlayer, for a total of 30 periods. (a) Sample A (conventional SB), where the interlayer is a fixed thickness. (b) Samples B–C: the first 15 periods contain approximately a 2 nm thick GaN interlayer. After the first 15 periods, the GaN interlayer was increased by 0.3 nm every three periods, ending in a final interlayer thickness of 3.5 nm.

targeting an indium content of x ~ 0.085, and sample C was grown at a higher temperature targeting x ~ 0.07. Periodicity was determined by x-ray diffraction (XRD) via $2\theta$-$\omega$ scans of the [00.2] direction. The thickness of the periods in conventional SB is ~21 nm. Atomic Force Microscopy (AFM) images were collected on an Asylum MFP-3D classic Atomic Force Microscope with a tip with a radius of <10 nm to study the surface morphology of the samples. High-Resolution XRD (HRXRD) rocking curves ($\omega$-scans) of the symmetric (00.2) and asymmetric (10.5) reflections for sample B were collected using a Rigaku SmartLab x-Ray Diffractometer in parallel beam geometry to estimate the dislocation density.

Sample C was used for measuring the etch pit density (EPD). The technique relies on treating the samples with $SiH_4$ in the presence of $NH_3$ at high temperatures, to increase the diameter of etch pits related to screw- and edge-type TDs, making it easier to detect them using AFM. This technique was reported by Oliver *et al.*[16] to study dislocation densities in GaN films. Applying such a technique directly to the InGaN template surface was not successful due to the thermal instabilities of InGaN at the high temperatures needed to delineate the etch pits. To overcome such a problem, in the current work, the InGaN templates were capped with a thin fully strained 10 nm GaN layer, where silane etching was performed. The thicknesses of these GaN cap layers are lower than the critical layer thickness (CLT);[17] thus, no additional defects are generated due to these capping layers. Thus, the EPD achieved in these capping GaN layers represents that of the underlying InGaN templates. For sample C, the 10 nm GaN cap layer was grown at 1025 C as a protective barrier for a later silane etch. PL measurements were performed before and after the deposition of the 10 nm GaN protective layer. After AFM, silane etching was performed at 860 C, and $H_2$ and 20 ppm $SiH_4$ at 5 sccm were flowed into the reactor for a total of 15 min.

PL emission for each sample can be seen in Fig. 2. The bandgap of $In_xGa_{1-x}N$ is dependent on the indium content as well as the degree of strain relaxation of the sample; thus, for a certain indium content, the emission can be used to estimate a range of degrees of relaxation at the topmost layers. The subject of the strain relaxation range in the SB templates is discussed elsewhere,[13,14] and we will utilize the strategy discussed in the study by Abdelhamid *et al.* for estimation of strain relaxation in the top layer using a combination of PL and secondary-ion mass spectrometry (SIMS).[14] It is important to note that the degree of relaxation of the topmost layer is an estimation, and the limitations of determining strain relaxation and x in the topmost layer of the semibulk templates are further discussed in the supplementary material. From previous work under similar growth conditions, we have seen from SIMS data that for a 30-period SB emitting at 429 nm, the indium content varies from x ~ 0.066 at the first few periods to x ~ 0.11 at the topmost period as the sample gradually relaxes with each successive period. The degree of relaxation at the topmost layer was estimated to be ~80%. For a 20-period SB emitting at 414 nm, the indium content varied form x ~ 0.066–0.092 with a degree of relaxation of ~60% at the topmost layer.[14]

Applying these previous results to the PL data of the current study, sample A is emitting at 411 nm corresponding to x ~ 0.085–0.09 with a degree of relaxation range of ~60%–70%. Sample B emits at 409 nm, indicating that slightly less relaxation occurred at the top layer for this growth due to the increased interlayer thickness. The GaN interlayers are subjected to tensile stresses. For sample C

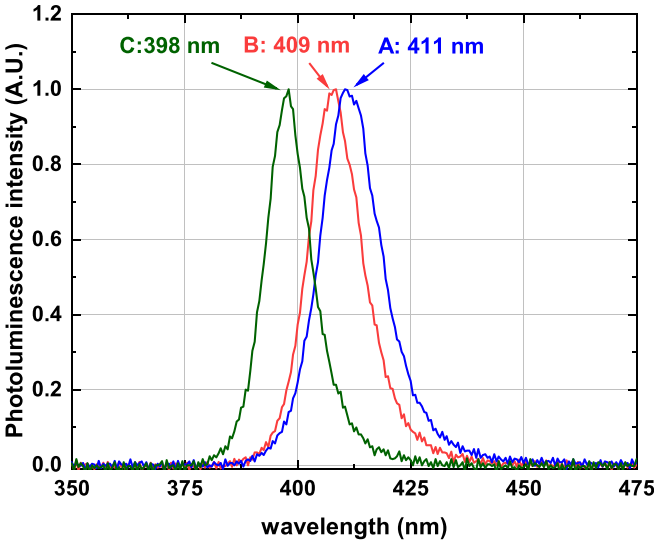


**FIG. 2.** Photoluminescence emission for samples A–C.

emitting at 398 nm, the indium content x ∼ 0.07 with a degree of relaxation range of ∼50%–60%.

The surface morphology of sample A and sample B can be compared in the AFM height retrace seen in Fig. 3. As seen in Fig. 3(a), sample A (conventional SB) displays large pitting and has a root mean square (RMS) surface roughness of approximately 9.20 nm. The pit density of the conventional SB is approximately $5 \times 10^7$ cm$^{-2}$; however, as seen in Fig. 3(a), as indicated with the line profile, the pits on the surface are large in diameter. Sample B (SB with the increasing interlayer thickness), as seen in Fig. 3(b), does not display similar pitting, but instead has smaller pits at the edges of terraces, with a pit density of approximately $2 \times 10^7$ cm$^{-2}$ and an improvement in smoothness, at a RMS roughness of 3.70 nm. When surveying $(1\ \mu m)^2$ areas of sample B, the RMS roughness is < 1 nm. The depth profile of the pit in sample A can be seen in Fig. 3(c), showing a pit depth of ∼25 nm with a diameter of ∼0.49 $\mu$m, whereas the depth of the pit in sample B, seen in Fig. 3(d), is ∼8 nm, with a diameter of ∼0.17 $\mu$m. The pit density of InGaN/GaN heterostructures prior to any surface

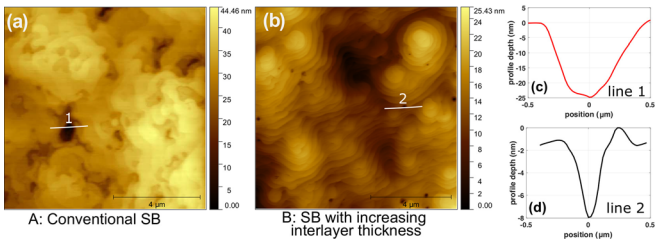


**FIG. 3.** (a) AFM height retrace of sample A, with an RMS roughness of 9.2 nm. The large pit (∼25 nm deep) is indicated with an arrow, (b) AFM height retrace of sample B, with an RMS roughness of 3.7 nm, with the smaller, shallower (∼8 nm deep) pits indicated with arrows. (c) The line profile of pit 1 in (a). (d) The line profile of pit 2 in (b).

treatment is reported to be $\sim 8 \times 10^7$ cm$^{-2}$.[9] The results of decreased *V-pit* on the surface with an increased GaN interlayer agree with Dussaigne *et al.*[15]

The edge and screw dislocations can be quantified by using the (00.2) and (10.5) reflections from HRXRD $\omega$-scans (HRXRD rocking curves).[18] GaN systems grown in the c-direction are prone to threading dislocations (TDs) with dislocations along the c-axis of the edge and screw variety due to misorientation during growth. The proportion of screw-type to edge-type dislocations varies,[18] but, in general, more edge-type dislocations are present in hexagonal GaN systems.[19]

Tilt (out-of-plane misorientation) is measured via (00.$\ell$) HRXRD rocking curves, and twist (in-plane misorientation) is measured via off-axis (hk. $\ell$) HRXRD rocking curves where h or k $\neq 0$.[18,20] For high dislocation density films, the mosaic model can be used to describe the dislocations in the film. However, for lower dislocation density films, a random distribution model should be assumed.[18] In the case of high dislocation density films (>$10^{10}$ cm$^{-2}$), the resulting peak profile can be described using a Gaussian model; however, for lower dislocation density films (<$5 \times 10^8$ cm$^{-2}$), the peak profile is more accurately described with a Pseudo-Voigt function.[18,20] The Pseudo-Voigt function "PV" is defined as[21,22]

$$PV(x) = I_0(\eta L(x) + (1-\eta)G(x)), \tag{1}$$

which is a weighted linear convolution of a Lorentzian fit, L(x), and a Gaussian fit, G(x), multiplied by a Lorentzian fit factor, $\eta$, and x is values of $\omega$. The details of the fit that follows Eq. (1) for each rocking curve can be seen in the supplementary material. Different skew symmetric reflections are used for the quantification of the edge-type dislocations via HRXRD rocking curves;[23–25] and (10.5) was chosen for this work due to the lack of distortion from the GaN sublayer rocking curve as well as a reasonable intensity. The dislocation density $D$ can be correlated with the HRXRD rocking curves obtained via the following relationships:[21,22,26]

$$D_{screw/edge} = \frac{\alpha_\theta^2}{2\pi \ln(2) b_{c/a}^2}, \tag{2}$$

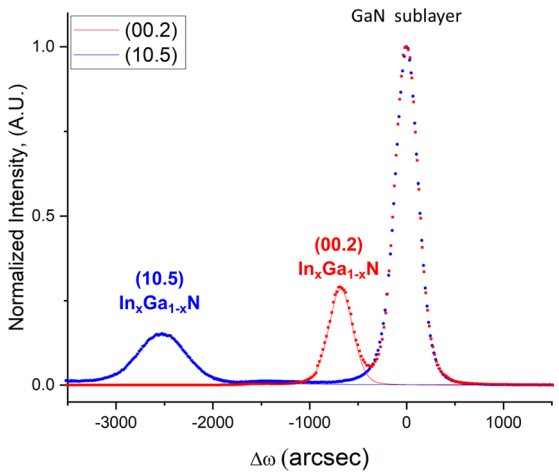


**FIG. 4.** Rocking curves ($\omega$-scans) of sample B of (00.2) (red) and (10.5) (blue) reflections, normalized to the GaN sublayer reflection.

**TABLE I.** Dislocation density obtained from (00.2) and (10.5) rocking curves for (sample B).

| | (00.2)/tilt/screw | (10.5)/twist/edge |
|---|---|---|
| Peak pos. relative to GaN, $\Delta\omega$ | −680 arc sec | −2529 arc sec |
| Integral breadth, $\beta$ | 332 arc sec | 799 arc sec |
| Rotational angle, $\alpha_\theta$ | 315 arc sec | 247 arc sec |
| Dislocation density, $D_{screw/edge}$ | $1.3 \times 10^8$ cm$^{-2}$ | $5.3 \times 10^8$ cm$^{-2}$ |

$$D_{total} = D_{screw} + D_{edge}, \tag{3}$$

where b is the burgers vector of $b_c = 0.5185$ nm and $b_a = 0.3189$ nm, for screw-type and edge-type dislocations, respectively.[23] The rotational angle, $\alpha_\theta$, is defined as

$$\alpha_\theta = \beta(0.184\,46 + 0.812\,692(1 - 0.998\,49\eta)^{\frac{1}{2}} - 0.659\,60\eta + 0.445\,54\eta^2), \tag{4}$$

where $\beta$ is the integral breadth of the measured $In_xGa_{1-x}N$ HRXRD rocking curve determined using a fitting software following Eq. (1).[23] The resulting HRXRD rocking curves can be seen in Fig. 4.

As seen in Table I, the (00.2) and (10.5) reflections are observed at −680 and −2529 arc sec, respectively.

The integral breadths are 332 arc sec for the (00.2) InGaN reflection and 799 arc sec for the (10.5) InGaN reflection, as seen in Table I. Using Eq. (2)–(4), the dislocation density can be obtained. For the screw-type dislocation density, it is found to be approximately $1.3 \times 10^8$ cm$^{-2}$ and $5.3 \times 10^8$ cm$^{-2}$ for edge-type dislocations. The screw-type and edge-type dislocation densities of the GaN reflection are found to be $1.2 \times 10^8$ cm$^{-2}$ and $2.7 \times 10^8$ cm$^{-2}$, consistent with the manufacturer's reported dislocation density of $\sim 10^8$ cm$^{-2}$.

Sample C was used to determine experimentally the etch pit density (EPD) and compare it with the dislocation densities obtained from HRXRD rocking curves. As seen in Figs. 5(a) and 5(c), the surface of sample C is smooth, with an RMS roughness of 1.108 nm across a $(5\ \mu m)^2$ area, as well as subnanometer for a $(1\ \mu m)^2$ area and has step flow growth mode prior to the treatment with silane. As seen in Table II, the pit densities are $1.3 \times 10^8$ cm$^{-2}$ for the $(2\ \mu m)^2$ area and $7.2 \times 10^7$ cm$^{-2}$ for the $(5\ \mu m)^2$ area, resulting in a weight average pit density of $8 \times 10^7$ cm$^{-2}$ prior to silane treatment. As seen in the $(2\ \mu m)^2$ area height retrace, a few pits are observed. Pits observed in pre-silane treatment samples are small in size and seen at the termination of steps, consistent with how screw-type dislocations are present.[16] As compared to Fig. 3, sample C exhibits a smooth surface with step-flow growth like sample B, indicating that the increasing interlayer thickness allows for a more efficient *V-pit* filling process.

The silane treatment results are listed in Table II. As discussed in the study by Oliver *et al.*, qualitative observations can be used to attribute edge-type and screw-type dislocations to the etched pits.[16] As seen in Figs. 5(b) and 5(d), the post treatment surface shows both an increase in the number of pits and an increase in the size of the pits. The $(5\ \mu m)^2$ area scan was used to determine the spread of the diameter for the pits. Figure 5(e) shows a histogram of the diameter of pits for sample C for the post-silane treatment $(5\ \mu m)^2$ area scan. Previous work by Oliver *et al.* shows a bimodal distribution of pit diameters post silane anneal.[16] Considering the grouping of the diameters, "large" pits were considered to be the diameters to the middle and far right of the histogram, corresponding to diameters greater than 98 nm, whereas "small" pits were considered pits corresponding to diameters lower than 73 nm, as seen in Fig. 5. If the small pits are correlated with edge dislocations and large pits to screw dislocations, then the resulting weighted averages for the edge-type EPD and screw-type EPD were $1.8 \times 10^8$ cm$^{-2}$ and $5.2 \times 10^7$ cm$^{-2}$, respectively, with a total EPD of $2.3 \times 10^8$ cm$^{-2}$.

The reliability of this silane etching approach was tested by comparing the silane etch EPD results with a known standard. A 290 nm GaN layer was grown on the commercially supplied GaN on sapphire with a reported dislocation density of $\sim 10^8$ cm$^{-2}$. Similar to the results of sample C, small pits and large pits were observed on the GaN standard. The resulting small EPD attributed to edge-type TDs was $9.2 \times 10^7$ cm$^{-2}$, and large EPD attributed to screw-type dislocations was $1 \times 10^8$ cm$^{-2}$, consistent with the manufacturer's total dislocation density of $\sim 10^8$ cm$^{-2}$. There is reasonable agreement between EPD obtained due to silane etching and dislocation density obtained from HRXRD rocking curves. InGaN templates can be grown epitaxially with defect densities comparable to good quality GaN.

Using a gradually increasing GaN interlayer thickness in our SB growth procedure, we are able to obtain device quality $In_xGa_{1-x}N$ (x ∼0.08) SB templates for MQW growth with low TD density and pit density. When compared to a conventional SB, the pit coalescence is minimized, and the pit density falls from $5 \times 10^7$ cm$^{-2}$ to $\sim 2 \times 10^7$ cm$^{-2}$. Screw-type and edge-type dislocations were characterized using the (00.2) and (10.5) reflections from high-resolution x-ray

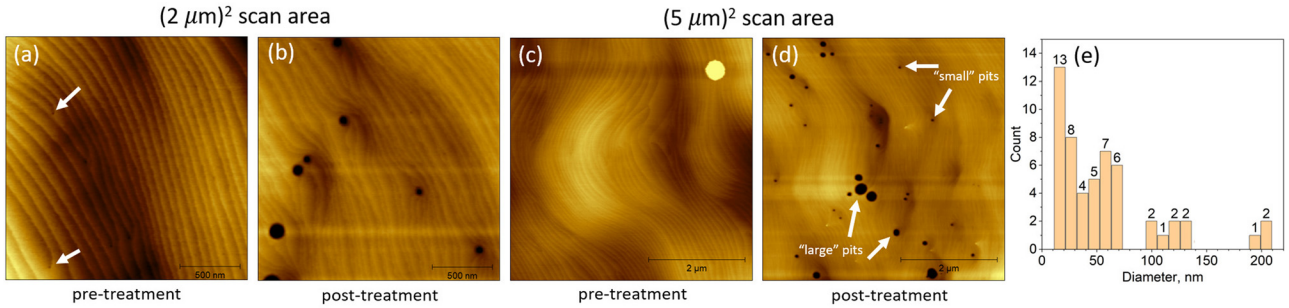


**FIG. 5.** AFM height retrace of sample C pre-silane treatment, post growth, where step flow is seen, and small pits are observed at the termination of step-edges, indicated by arrows. (b) AFM height retrace of sample C, post silane treatment. An increase in the number of pits is observed, as well as an increase in the pit diameter in both scan areas.

**TABLE II.** Etch pit density determined via AFM and silane etching for sample C.

| | | $(2\ \mu m)^2$ scan area Pre-treatment | Post-treatment | $(5\ \mu m)^2$ scan area Pre-treatment | Post-treatment | Weighted average |
|---|---|---|---|---|---|---|
| Small pits | Count | 5 | 6 | 18 | 43 | … |
| | Pit density | $1.3 \times 10^8$ cm$^{-2}$ | $1.5 \times 10^8$ cm$^{-2}$ | $7.2 \times 10^7$ cm$^{-2}$ | $1.8 \times 10^8$ cm$^{-2}$ | $1.8 \times 10^8$ cm$^{-2}$ |
| Large pits | Count | … | 5 | … | 10 | … |
| | Pit density | … | $1.3 \times 10^8$ cm$^{-2}$ | … | $4.0 \times 10^7$ cm$^{-2}$ | $5.2 \times 10^7$ cm$^{-2}$ |
| Total pits | Count | 5 | 11 | 18 | 53 | … |
| | Pit density | $1.3 \times 10^8$ cm$^{-2}$ | $2.8 \times 10^8$ cm$^{-2}$ | $7.2 \times 10^7$ cm$^{-2}$ | $2.2 \times 10^8$ cm$^{-2}$ | $2.3 \times 10^8$ cm$^{-2}$ |

rocking curve omega-scans, respectively. The total dislocation density obtained via RCs was found to be $6.6 \times 10^8$ cm$^{-2}$, with the screw-type and edge-type being $1.3 \times 10^8$ cm$^{-2}$ and $5.3 \times 10^8$ cm$^{-2}$, respectively. The pit density was determined via AFM. The SB templates with the gradually increasing GaN interlayers were found to have an EPD in the range of $2.3 \times 10^8$ cm$^{-2}$. When correlating the size of the diameters (small and large) of the etch pits with screw-type and edge-type dislocations, the EPD was determined to be $5.2 \times 10^7$ cm$^{-2}$ and $1.8 \times 10^8$ cm$^{-2}$, respectively, which is consistent with the dislocation density reported for the commercially supplied GaN buffer ($1 \times 10^8$ cm$^{-2}$). The values of the EPD and the dislocation densities obtained from the HRXRD rocking curve are in reasonable agreement. However, the EPD approach of the TD density measurement allows for faster turnaround during calibration of templates for growth for devices.

See the supplementary material for detail on the estimation of strain relaxation in the semibulk samples, as well as detail on the curve fitting used for the HRXRD rocking curves.

We would like to acknowledge The Analytical Instrumentation Facility at NCSU for XRD and AFM for support. N. A. El-Masry would like to acknowledge the National Science Foundation IRD program. This work was supported by National Science Foundation Grant Nos. ECCS-1407772 and ECCS-1833323.

## DATA AVAILABILITY

The data that support the findings of this study are available within this article and its supplementary material.

## REFERENCES

[1]S. Saito, R. Hashimoto, J. Hwang, and S. Nunoue, "InGaN light-emitting diodes on c-face sapphire substrates in green gap spectral range," Appl. Phys. Express **6**, 111004 (2013).
[2]P. T. Barletta, E. A. Berkman, B. F. Moody, N. A. El-Masry, A. M. Emara, M. J. Reed, and S. M. Bedair, "Development of green, yellow, and amber light emitting diodes using InGaN multiple quantum well structures," Appl. Phys. Lett. **90**, 151109 (2007).
[3]Z. Liliental-Weber, M. Benamara, J. Washburn, J. Z. Domagala, J. Bak-Misiuk, E. L. Piner, J. C. Roberts, and S. M. Bedair, "Relaxation of InGaN thin layers observed by X-ray and transmission electron microscopy studies," J. Electron. Mater. **30**, 439–444 (2001).
[4]H. K. Cho, J. Y. Lee, G. M. Yang, and C. S. Kim, "Formation mechanism of V defects in the InGaN/GaN multiple quantum wells grown on GaN layers with low threading dislocation density," Appl. Phys. Lett. **79**, 215–217 (2001).
[5]M. F. Schubert, S. Chhajed, J. K. Kim, E. F. Schubert, D. D. Koleske, M. H. Crawford, S. R. Lee, A. J. Fischer, G. Thaler, and M. A. Banas, "Effect of dislocation density on efficiency droop in GaInNGaN light-emitting diodes," Appl. Phys. Lett. **91**, 231114 (2007).
[6]D. Van Den Broeck, D. Bharrat, Z. Liu, N. El-Masry, and S. Bedair, "Growth and characterization of high-quality, relaxed $In_yGa_{1-y}N$ templates optoelectronic applications," J. Electron. Mater. **44**, 4161–4166 (2015).
[7]T. Song, S. Chua, and E. Fitzgerald, "Effect of dislocation density on efficiency droop in GaInNGaN light-emitting diodes," J. Vac. Sci. Technol., A **22**, 287–292 (2004).
[8]J. Däubler, T. Passow, R. Aidam, K. KÖhler, L. Kirste, M. Kunzer, and J. Wagner, "Long wavelength emitting GaInN quantum wells on metamorphic GaInN buffer layers with enlarged in-plane lattice parameter," Appl. Phys. Lett. **105**, 111111 (2014).
[9]S. Alam, S. Sundaram, M. Elouneg-Jamroz, X. Li, Y. E. Gmili, I. C. Robin, P. L. Voss, J.-P. Salvestrini, and A. Ougazzaden, "InGaN/InGaN multiple-quantum-well grown on InGaN/GaN semi-bulk buffer for blue to cyan emission with improved optical emission and efficiency droop," Superlattices Microstruct. **104**, 291–297 (2017).
[10]A. Lochthofen, W. Mertin, G. Bacher, L. Hoeppel, S. Bader, J. Off, and B. Hahn, "Electrical investigation of v-defects in GaN using Kelvin probe and conductive atomic force microscopy," Appl. Phys. Lett. **93**, 022107 (2008).
[11]S. Mahanty, M. Hao, T. Sugahara, R. S. Fareed, Y. Morishima, Y. Naoi, T. Wang, and S. Sakai, "V-shaped defects in InGaN/GaN multiquantum wells," Mater. Lett. **41**, 67–71 (1999).
[12]M. Shiojiri, C. C. Chuo, J. T. Hsu, J. R. Yang, and H. Saijo, "Structure and formation mechanism of V defects in multiple InGaN/GaN quantum well layers," J. Appl. Phys. **99**, 073505 (2006).
[13]T. B. Eldred, M. Abdelhamid, J. G. Reynolds, N. A. El-Masry, J. M. Lebeau, and S. M. Bedair, "Observing relaxation in device quality InGaN templates by TEM techniques," Appl. Phys. Lett. **116**, 102104 (2020).
[14]M. Abdelhamid, J. G. Reynolds, N. A. El-Masry, and S. M. Bedair, "Growth and characterization of $In_xGa_{1-x}N$ ($0 < x < 0.16$) templates for controlled emissions from MQW," J. Cryst. Growth **520**, 18–26 (2019).
[15]A. Dussaigne, F. Barbier, B. Samuel, A. Even, R. Templier, F. Lévy, O. Ledoux, M. Rozhavskaia, and D. Sotta, "X-ray diffraction of III-nitrides," J. Cryst. Growth **533**, 125481 (2020).
[16]R. Oliver, M. Kappers, J. Sumner, R. Datta, and C. Humphreys, "Highlighting threading dislocations in MOVPE-grown GaN using an in situ treatment with $SiH_4$ and $NH_3$," J. Cryst. Growth **289**, 506–514 (2006).
[17]M. J. Reed, N. A. El-Masry, C. A. Parker, J. C. Roberts, and S. M. Bedair, "Critical layer thickness determination of GaN/InGaN/GaN double heterostructures," Appl. Phys. Lett. **77**, 4121–4123 (2000).
[18]M. A. Moram and M. E. Vickers, "X-ray diffraction of III-nitrides," Rep. Prog. Phys. **72**, 036502 (2009).
[19]R. Datta, M. Kappers, M. E. Vickers, J. S. Barnard, and C. J. Humphreys, "Growth and characterisation of GaN with reduced dislocation density," Superlattices Microstruct. **36**, 393–401 (2004).
[20]M. E. Vickers, M. J. Kappers, R. Datta, C. McAleese, T. M. Smeeton, F. D. Rayment, and C. J. Humphreys, "In-plane imperfections in GaN studied by x-ray diffraction," J. Phys. D: Appl. Phys. **38**, A99 (2005).
[21]T. Metzger, R. Hopler, E. Born, O. Ambacher, M. Stutzmann, R. Stömmer, M. Schuster, H. Göbel, S. Christiansen, M. Albrecht, and H. P. Strunk, "Defect

structure of epitaxial GaN films determined by transmission electron microscopy and triple-axis x-ray diffractometry," Philos. Mag. A **77**, 1013–1025 (1998).
[22]Q. Wang, J. Yang, Y. Wei, W. Fang, and L. He, "Evaluation of dislocation densities in HgCdTe films by high-resolution x-ray diffraction," Proc. SPIE **5640**, 629 (2005).
[23]M. K. Öztürk, S. Çörekçi, M. Tamer, S. S. Çetin, S. Özçelik, and E. Özbay, "Microstructural properties of InGaN/GaN light-emitting diode structures with different in content grown by MOCVD," Appl. Phys. A **114**, 1215–1221 (2014).
[24]J. F. Zhang, Y. H. Nie, Y. B. Zhou, K. Tian, W. Ha, M. Xiao, J. C. Zhang, and Y. Hao, "Depth-dependent mosaic tilt and twist in GaN epilayer: An approximate evaluation," Chin. Phys. B **23**, 068102 (2014).
[25]D. Chidambaram, G. Vattikondala, G. Marappan, and Y. Sivalingam, "Indium content dependent VOCs interactions in monolithic InGaN/GaN multi quantum well structures grown by MOCVD," Mater. Sci. Semicond. Process. **104**, 104694 (2019).
[26]C. G. Dunn and E. F. Kogh, "Comparison of dislocation densities of primary and secondary recrystallization grains of Si-Fe," Acta Metall. **5**, 548–554 (1957).